# Photochemistry and Emission of the Dinuclear Complexes $(CO)_5MnRe(CO)_3(L)$ (L = 2,2′-Bipyrimidine, 2,3-Bis(2-pyridyl)pyrazine) and Bridged Trinuclear Complexes $(CO)_5MnRe(CO)_3(L)Re(Br)(CO)_3$ and $(CO)_5MnRe(CO)_3(BPYM)W(CO)_4$: Effect of the Remote Metal Center on the Photodissociation of the Mn−Re Bond

**J. W. M. van Outersterp and D. J. Stufkens***

Anorganisch Chemisch Laboratorium, Universiteit van Amsterdam, J. H. van't Hoff Research Instituut, Nieuwe Achtergracht 166, 1018 WV Amsterdam, The Netherlands

**A. Vlček, Jr.***

J. Heyrovský Institute of Physical Chemistry, Academy of Sciences of the Czech Republic, Dolejškova 3, 18223 Prague, Czech Republic

*Received February 9, 1995*[⊗]

Photochemical and emission properties of the dinuclear $(CO)_5MnRe(CO)_3(L)$ and trinuclear $(CO)_5MnRe(CO)_3(L)Re(Br)(CO)_3$ and $(CO)_5MnRe(CO)_3(BPYM)W(CO)_4$ complexes (L = 2,2′-bipyrimidine (BPYM), 2,3-bis(2-pyridyl)pyrazine (DPP)) are described. All these compounds undergo photochemical homolysis of the Mn−Re bond upon excitation into their MLCT absorption band(s) in the visible spectral region. $Mn(Cl)(CO)_5$ and $Re(Cl)(CO)_3(L)$ or $Re(Cl)(CO)_3(L)Re(Br)(CO)_3$ are formed in chlorinated solvents ($CH_2Cl_2$, $CCl_4$) from the former two types of complexes, respectively. In THF, photolysis produces $Mn_2(CO)_{10}$, together with $[Re(CO)_3(L)]^•$, $[Re(CO)_3(L)Re(Br)(CO)_3]^•$, or $[Re(CO)_3(BPYM)W(CO)_4]^•$ radicals, respectively, which presumably contain also a coordinated THF molecule. Photoreactions of the dinuclear complexes occur with high quantum yields (0.36 for BPYM and 0.54 for DPP), which are independent of the temperature and of the excitation wavelength. The attachment of the $Re(Br)(CO)_3$ group to the potentially bridging ligand L in $(CO)_5MnRe(CO)_3(L)$ to form the L-bridged trinuclear species strongly influences the excited state dynamics involved in the photochemistry. Thus, the photochemical quantum yields of the trinuclear complexes are both temperature and excitation wavelength dependent. The apparent activation energy, together with the overall quantum yield, decreases upon changing the excitation from the high- to the low-energy MLCT absorption band. The Mn−Re bond homolysis is about 6 times more efficient for bridging DPP than for bridging BPYM. The dinuclear complexes exhibit, in a 2-MeTHF glass at 80 K, an emission from thermally unequilibrated states, whereas double emission, extending into the near-IR spectral region, was observed for $(CO)_5MnRe(CO)_3(DPP)Re(Br)(CO)_3$. Its BPYM analogue is nonemissive. To account for this complex photobehavior, an excited state diagram and a qualitative dynamics model are proposed. The reaction is assumed to occur from a $^3\sigma\pi^*$ state that is nonradiatively populated from the higher MLCT state(s). The main effects of the attachment of the $Re(Br)(CO)_3$ group, which is responsible for the changed photochemical behavior, are the profound stabilization of the $\pi^*$ LUMO of the bridging ligand L and the introduction of another MLCT excited state into the trinuclear molecule.

## Introduction

Ligand-bridged polynuclear complexes often exhibit very interesting spectroscopic, photophysical, and photochemical properties[1,2] which, in most cases, differ significantly from those of their mononuclear components. Both the nature and magnitude of these differences depend very much on the extent and mechanism of the electronic coupling between the metal centers in the bridged complexes, in both their ground and their electronically excited states. For example, the amply studied dinuclear complexes bridged by aromatic nitrogen heterocycles[1−3] exhibit the metal-to-bridging ligand charge transfer (MLCT) transitions at much lower energies[2,4−16] than their mononuclear components, due to a significant stabilization of the $\pi^*$ orbitals of the ligand upon its simultaneous coordination to two metal

* To whom correspondence should be addressed.

[⊗] Abstract published in *Advance ACS Abstracts,* September 1, 1995.

(1) Balzani, V.; Scandola, F. *Supramolecular Chemistry*; Ellis Horwood: Chichester, U.K., 1991.
(2) Scandola, F.; Indelli, M. T.; Chiorboli, C.; Bignozzi, C. A. *Topics in Current Chemistry*; Springer-Verlag: Berlin, Heidelberg, 1990; Vol. 158; p 73.
(3) Steel, P. J. *Coord. Chem. Rev.* **1990**, *106*, 227.
(4) Rillema, D. P.; Mack, K. B. *Inorg. Chem.* **1982**, *21*, 3849.
(5) Ruminski, R. R.; Petersen, J. D. *Inorg. Chem.* **1982**, *21*, 3706.
(6) Braunstein, C. H.; Baker, A. D.; Strekas, T. C.; Gafney, H. D. *Inorg. Chem.* **1984**, *23*, 857.
(7) Fuchs, Y.; Lofters, S.; Dieter, T.; Shi, W.; Morgan, R.; Strekas, T. C.; Gafney, H. D.; Baker, A. D. *J. Am. Chem. Soc.* **1987**, *109*, 2691.
(8) Brewer, K. J.; Murphy, W. R., Jr.; Petersen, J. D. *Inorg. Chem.* **1987**, *26*, 3376.
(9) Ruminski, R. R.; Cockroft, T.; Shoup, M. *Inorg. Chem.* **1988**, *27*, 4026.
(10) Sahai, R.; Rillema, D. P.; Shaver, R.; van Wallendael, S.; Jackman, D. C.; Boldaij, M. *Inorg. Chem.* **1989**, *28*, 1022.
(11) Kalyanasundaram, K.; Nazeeruddin, M. K. *J. Chem. Soc., Dalton Trans.* **1990**, 1657.
(12) Ruminski, R.; Cambron, R. T. *Inorg. Chem.* **1990**, *29*, 1575.
(13) van Wallendael, S.; Shaver, R. J.; Rillema, D. P.; Yoblinski, B. J.; Stathis, M.; Guarr, T. F. *Inorg. Chem.* **1990**, *29*, 1761.
(14) Matheis, W.; Kaim, W. *Inorg. Chim. Acta* **1991**, *181*, 15.
(15) Yoblinski, B. J.; Stathis, M.; Guarr, T. F. *Inorg. Chem.* **1992**, *31*, 5.
(16) Kaim, W.; Kohlmann, S.; Lees, A.; Snoeck, T. L.; Stufkens, D. J.; Zulu, M. M. *Inorg. Chim. Acta* **1993**, *210*, 159.

0020-1669/95/1334-5183$09.00/0 

centers. As these MLCT transitions have rather large oscillator strengths, di or polynuclear complexes containing bridging MLCT-active ligands often absorb effectively even low-energy visible light and may thus function as light-energy collecting "antenna" molecules.[1,2] Harvested excitation energy may be transferred to another component of the polynuclear complex where it is "utilized" by inducing chemical transformation, electron transfer, or photon emission.[1,2] Molecules with a chromophoric center linked to a reactive, potentially catalytic metal center are of special chemical interest. Complexes like $[(BPY)_2Ru(\mu\text{-}L)RhH_2(PPh_3)_2]^{3+}$ or $\{[(BPY)_2Ru(\mu\text{-}L)]_2MCl_2\}^{n+}$ ($M = Ir^{III}$, $Rh^{III}$, $Os^{II}$) might serve as examples.[17-19] The above mentioned stabilization of the bridging ligand $\pi^*$ orbitals is also responsible for rather positive reduction potentials exhibited by many polynuclear bridged complexes.

Lifetimes and emission properties of MLCT excited states of dinuclear transition metal carbonyls bridged by aromatic nitrogen heterocycles depend strongly on the nature of the bridging ligand. Thus, most dinuclear complexes bridged by the 2,2′-bipyrimidine ligand, BPYM, like $[Re(Cl)(CO)_3(BPYM)Re(Cl)(CO)_3]$, $[(BPY)_2Ru(BPYM)Re(Cl)(CO)_3]^{2+}$, or $[(BPY)_2Ru(BPYM)Ru(BPY)_2]^{4+}$, either are nonemissive or emit very weakly at 77 K, although their mononuclear components $Re(Cl)(CO)_3(BPYM)$ and $[Ru(BPY)_2(BPYM)]^{2+}$ are strongly emitting at room temperature in fluid solutions.[2,6,7,10,11,13,20-22] On the other hand, analogous complexes bridged by 2,3-bis(2-pyridyl)pyrazine (DPP) are emissive from their low-lying MLCT excited states already at room temperature in solutions.[2,11,13,15,23] The lack of emission for the bridged BPYM complexes has originally been explained by assuming either a relatively strong metal−metal coupling through the BPYM ligand[6,21] or an intervening intervalence state.[20] However, another explanation[7] takes into account the stabilization of the $\pi^*$ orbitals that is much larger for BPYM than for the other bridging ligands, including DPP. Hence, the MLCT excited state energy of dinuclear BPYM complexes is rather low and the emission may occur in the near-infrared region with a short lifetime, according to the energy gap law. This explanation looks rather plausible, being supported by the observation[10] of long-lived room-temperature emissions from tri- and tetranuclear complexes $[(BPY)Ru\{(BPYM)Re(Cl)(CO)_3\}_2]^{2+}$, $\tau$ = 942 ns, and $[Ru\{(BPYM)Re(Cl)(CO)_3\}_3]^{2+}$, $\tau$ = 847 ns, that occur at relatively high energies: 630 and 640 nm, respectively. On the other hand, the low-energy emission (774 nm) of analogous $[(BPY)_2Ru(BPYM)Re(Cl)(CO)_3]^{2+}$ is weak and observable in a low-temperature (77 K) glass only. Moreover, contrary to the assumption involved in the early explanations[6,20,21] of different emission properties of dinuclear DPP and BPYM complexes, the metal−metal coupling through the $\pi$ system of the pyrazine ring of the DPP ligand is expected to be stronger than that through the pyrimidine rings of BPYM, whose nitrogen donor atoms are in unfavorable meta positions.[24,25]

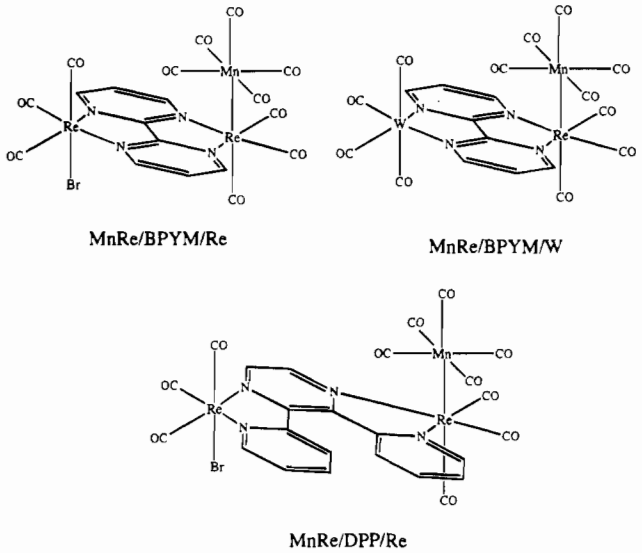


**Figure 1.** Schematic drawings of the complexes MnRe/L/Re (L = BPYM, DPP) and MnRe/BPYM/W.

Recently, we described the spectroscopic[26] and electrochemical[27,28] properties of the trinuclear complexes $(CO)_5MnRe(CO)_3(L)Re(Br)(CO)_3$ (L = BPYM, DPP) and $(CO)_5MnRe(CO)_3(BPYM)W(CO)_4$, which will hereafter be abbreviated as MnRe/L/Re and MnRe/BPYM/W, respectively. Their general structures are shown in Figure 1. These species represent a new type of polynuclear complex, for a dinuclear $(CO)_5MnRe(CO)_3$ fragment with a direct Mn−Re single bond is linked, through a BPYM or DPP bridge, to another metal-containing fragment, $Re(Br)(CO)_3$ or $W(CO)_4$. All these species exhibit[26] two intense absorption bands in the visible region which were shown by resonance Raman spectroscopy to correspond to localized MLCT transitions from the $(CO)_5MnRe(CO)_3$ moiety and from $Re(Br)(CO)_3$ or $W(CO)_4$ unit to the bridging ligand. Hence, the interaction between the two metal-containing fragments in MnRe/L/Re and MnRe/L/W complexes must be rather weak in both the ground and MLCT excited states and the $MnRe^0/L/Re^I$ species might be viewed as class II[29] mixed-valence compounds. Moreover, the bridging BPYM ligand in MnRe/BPYM/Re was found[26] to be distorted by a simultaneous coordination to two metal atoms with different bonding properties. This distortion does not occur[26] for MnRe/DPP/Re, indicating stronger $MnRe^0$-$Re^I$ interaction through the pyrazine ring of DPP. Compared with those of the corresponding components, MnRe/L and $Re(Br)(CO)_3(L)$ or $W(CO)_4(L)$, the $\pi^*$ levels of the ligands L (L = BPYM, DPP) are stabilized upon formation of the bridged species. This effect is much stronger for BPYM than for DPP. As a consequence, the stable $[MnRe/BPYM/Re]^{\bullet-}$ radical anion, which contains bridging $[BPYM]^{\bullet-}$, is formed upon one-electron reduction of MnRe/BPYM/Re, whereas analogous $[MnRe/DPP/Re]^{\bullet-}$ undergoes heterolytic splitting of the Mn−Re bond.[27,28]

Considering that $(CO)_5MM'(CO)_3(\alpha\text{-diimine})$ complexes (M, M′ = Mn, Re) undergo efficient photochemical homolysis of the Mn−Re bond and that they, as well as $Re(Br)(CO)_3(L)$, are

(17) MacQueen, D. B.; Petersen, J. D. *Inorg. Chem.* **1990**, *29*, 2313.
(18) Bridgewater, J. S.; Vogler, L. M.; Molnar, S. M.; Brewer, K. J. *Inorg. Chim. Acta* **1993**, *208*, 179.
(19) Molnar, S. M.; Jensen, G. E.; Vogler, L. M.; Jones, S. W.; Laverman, L.; Bridgewater, J. S.; Richter, M. M.; Brewer, K. J. *J. Photochem. Photobiol., A* **1994**, *80*, 315.
(20) Vogler, A.; Kisslinger, J. *Inorg. Chim. Acta* **1986**, *115*, 193.
(21) Juris, A.; Campagna, S.; Bidd, I.; Lehn, J. M.; Ziessel, R. *Inorg. Chem.* **1988**, *27*, 4007.
(22) Kaim, W.; Kramer, H. E. A.; Vogler, C.; Rieker, J. *J. Organomet. Chem.* **1989**, *367*, 107.
(23) Baiano, J. A.; Carlson, D. L.; Wolosh, G. M.; DeJesus, D. E.; Knowles, C. F.; Szabo, E. G.; Murphy, W. R. *Inorg. Chem.* **1990**, *29*, 2327.
(24) Richardson, D. E.; Taube, H. *J. Am. Chem. Soc.* **1983**, *105*, 40.
(25) Larsson, S. *J. Am. Chem. Soc.* **1981**, *103*, 4034.
(26) van Outersterp, J. W. M.; Stufkens, D. J.; Fraanje, J.; Goubitz, K.; Vlček, A., Jr. *Inorg.Chem.* **1995**, *34*, 4756.
(27) van Outersterp, J. W. M.; Hartl, F.; Stufkens, D. J. *Inorg. Chem.* **1994**, *33*, 2711.
(28) van Outersterp, J. W. M.; Hartl, F.; Stufkens, D. J. *Organometallics* **1995**, *14*, 3303.
(29) Robin, M. B.; Day, P. *Advances in Inorganic Chemistry and Radiochemistry*; Academic Press: New York and London, 1967; Vol. 10.

known to be emissive,[30−40] it becomes obvious that the photophysics and photochemistry of the trinuclear MnRe/L/Re complexes present a challenging problem. Understanding of the emission and, especially, photoreactivity of these trinuclear species might provide more detailed information on the mutual influence of the $(CO)_5MnRe(CO)_3$ and $Re(Br)(CO)_3$ metal fragments, especially the internal conversion between the optically excited MLCT and the reactive $\sigma\pi^*$ states, the latter involving excitation of an electron from the $\sigma$(Mn−Re) orbital to the $\pi^*$ orbital of the bridging ligand. An answer to a more general question, whether a low-energetic excitation into the low-lying MLCT-excited states, characteristic of bridged polynuclear complexes, can bring about homolysis of the metal−metal bond, might have broader implications for a design of photocatalytic and photoinitiated processes. Therefore, we have investigated the photochemical reactivity and emissive properties of the MnRe/L/Re and MnRe/BPYM/W species and related them to their spectroscopic and electrochemical behavior. For comparison, the dinuclear MnRe/L species were investigated as well.

## Experimental Section

**Materials and Preparations.** The solvents 2-MeTHF (Merck) and THF (Jansen), used for the photochemical reactions, were distilled from Na wire under a $N_2$ atmosphere. $CCl_4$ and $CH_2Cl_2$ were distilled from $CaH_2$ under $N_2$. The ligands BPY (Merck), BPYM (Johnson & Matthey), and DPP (Aldrich) were used as received.

The complexes MnRe/L (L = BPY, BPYM, DPP),[30,41] MnRe/L/Re (L = BPYM, DPP),[26] and MnRe/BPYM/W[26] were synthesized according to literature procedures and purified by column chromatography on Silica 60, activated by heating overnight under vacuum at 180 °C, by elution with a gradient solution of THF and hexane.

**Spectroscopic Measurements and Instrumentation.** UV−vis absorption spectra were recorded on a Varian Cary 4E or Perkin-Elmer Lambda 5 spectrophotometer. FTIR spectra were measured using either a Nicolet 7199 B FTIR or a BioRad FTS-7 infrared spectrometer (16 scans, resolution 2 $cm^{-1}$). Low-temperature IR and UV−vis measurements were performed using an Oxford Instruments DN 1704/54 liquid-nitrogen-cooled cryostat with $CaF_2$ and quartz windows, respectively. Excitation spectra were recorded on a Spex Fluorolog II emission spectrometer. ESR spectra were recorded on a Varian E6 X-band spectrometer with a 100 kHz modulation.

All sample preparations for photochemical experiments were performed under an atmosphere of purified nitrogen, using Schlenck techniques. The solutions were carefully handled in the dark before performing the experiments. For the photochemical experiments, the solutions were irradiated in the cuvette or IR cell with the lines of a Spectra Physics SP 2025 argon ion laser.

Quantum yields for the disappearance of the parent complex were determined by measuring the decay of the visible absorption band on a Varian Cary 4E spectrophotometer using automatized procedures. The sample solutions were kept in thermostated cuvettes within the spectrophotometer during the measurements. Magnetically stirred sample solutions were irradiated through an optical fiber using the lines of either an SP Model 2016 or 2025 argon ion laser for the wavelength region 457.9−514.5 nm or a Coherent CR 590 dye laser with Coumarin, Rhodamine B, or DCM as a dye to cover the ranges 530−550, 560−610, and 620−655 nm, respectively. The light intensities of the argon ion laser lines were measured with a power meter (Coherent Model 212), which was calibrated with an Aberchrome 540P solution according to literature methods.[42] For the measurements with the dye lasers, use was made of a quantum counter (Applied Photophysics) which was calibrated with Aberchrome 540P,[42] Aberchrome 999P,[43] or Mesodiphenyl Helianthrene/Methylene Blue[44] for the ranges 530−550, 560−610, and 620−655 nm, respectively. The incident light intensity for all irradiation wavelengths was in the range between 1.5 and 2.5 mW. Absorption spectra of the photolyzed solution were measured automatically after preset irradiation time intervals. The light beam was blocked by a computer-controlled mechanical shutter during the measurement of the absorption spectra. The calculation of the quantum yields took fully into account the small changes of the partial light absorption by the photoactive compound during the irradiation. For quantum yield measurements, the total photochemical conversion was kept below 2%.

Sample solutions for emission measurements in freshly distilled 2-MeTHF were freeze−pump−thaw degassed at least four times and then sealed under vacuum. The low-temperature emission measurements were performed in an Oxford Instruments liquid-nitrogen-cooled cryostat using a cylindric, glass inner tube of 1 cm diameter as a cuvette. Emission spectra and lifetimes were obtained using a Spectra Physics GCR-3 Nd:YAG laser or a Quanta-Ray PDL-3 pulsed dye laser (Spectra Physics) as the excitation source. The emission was analyzed using an EG&G OMAIII handling system. Samples were excited either with 532 nm laser pulses (fwhm = 5 ns, maximum frequency 10 Hz) of the Nd:YAG laser or with 460 nm pulses of the dye laser that was pumped by the third harmonics of the Nd:YAG laser at 355 nm. The emitted light was focused on an optical fiber positioned perpendicularly to the excitation beam and transferred to a spectrograph (EG&G model 1234) equipped with a 150 g/mm grating and a 250 $\mu$m slit resulting in a resolution of 6 nm. This spectrograph was coupled to a gated, intensified diode array detector (EG&G Model 1421). The resulting signal was amplified by a 1304 gate pulse amplifier with variable time windows of 100 ns−10 ms or a 1303 gate pulse amplifier with a 5 ns gate window. The programming of the OMA enabled the measurement of time-resolved emission spectra at a given time delay after the excitation pulse. The 100 ns gate of the 1304 was used for the lifetime measurements. The lifetimes were determined from the emission spectra measured at 20 different delay times by fitting the emission signal at three different wavelengths of the emission band to first-order kinetics.

Emission quantum yields ($\Phi_{em}$) were measured using optically dilute solutions relative to a standard solution of $[Re(Cl)(CO)_3(BPY)]$ ($\Phi_s = 0.28 \times 10^{-1}$ at 77 K),[45] using the 10 ms gate. Corrections were made according to eq 1,[46,47] in which $\Phi$ is the quantum yield of the unknown

$$\Phi_u = \Phi_s\left(\frac{I_u}{I_s}\right)\left(\frac{A_s}{A_u}\right)\left(\frac{\eta_u}{\eta_s}\right)^2 \quad (1)$$

(u) and standard (s) emitting species, respectively, $I$ is the integrated emission intensity, $A$ is the ground-state absorbance at the excitation wavelength, and $\eta$ is the refractive index of the solvent.

## Results

The photochemistry of all complexes was studied at room temperature in different solvents. The course of the reactions

(30) Morse, D. L.; Wrighton, M. S. *J. Am. Chem. Soc.* **1976**, *98*, 3931.
(31) Stufkens, D. J. *Coord. Chem. Rev.* **1990**, *104*, 39.
(32) Stufkens, D. J. *Comments Inorg. Chem.* **1992**, *13*, 359.
(33) Rossenaar, B. D.; Lindsay, E.; Stufkens, D. J.; Vlček, A., Jr. *Inorg. Chim. Acta*, submitted.
(34) Glezen, M. M.; Lees, A. J.; Snoeck, T. L.; Stufkens, D. J. To be published.
(35) Larson, L. J.; Oskam, A.; Zink, J. I. *Inorg. Chem.* **1991**, *30*, 42.
(36) Andréa, R. R.; de Lange, W. G. J.; van der Graaf, T.; Rijkhoff, M.; Stufkens, D. J.; Oskam, A. *Organometallics* **1988**, *7*, 1100.
(37) Kokkes, M. W.; de Lange, W. G. J.; Stufkens, D. J.; Oskam, A. *J. Organomet. Chem.* **1985**, *294*, 59.
(38) Kokkes, M. W.; Stufkens, D. J.; Oskam, A. *Inorg. Chem.* **1985**, *24*, 2934.
(39) Kokkes, M. W.; Stufkens, D. J.; Oskam, A. *Inorg. Chem.* **1985**, *24*, 4411.
(40) van der Graaf, T.; Stufkens, D. J.; Oskam, A.; Goubitz, K. *Inorg. Chem.* **1991**, *30*, 599.
(41) Staal, L. H.; van Koten, G.; Vrieze, K. *J. Organomet. Chem.* **1979**, *175*, 73.
(42) Heller, H. G.; Langan, J. R. *J. Chem. Soc., Perkin Trans. 2* **1981**, 341.
(43) Kuhn, H. J.; Braslavsky, S. E.; Schmidt, R. *Pure Appl. Chem.* **1989**, *61*, 187.
(44) Adick, H. J.; Schmidt, R.; Brauer, H. D. *J. Photochem. Photobiol., A* **1989**, *49*, 311.
(45) Worl, L. A.; Duesing, R.; Chen, P.; Della Ciana, L.; Meyer, T. J. *J. Chem. Soc., Dalton Trans.* **1991**, 849.
(46) Caspar, J. V.; Meyer, T. J. *J. Am. Chem. Soc.* **1983**, *105*, 5583.
(47) Parker, C. A.; Rees, W. T. *Analyst (London)* **1960**, *85*, 587.

**Table 1.** IR and UV−Vis Data for MnRe/L and MnRe/L/Re (L = BPYM, DPP), MnRe/BPYM/W, and Their Photoproducts in Various Media

| complex | solvent | $T$ (K) | $\nu$(CO) (cm$^{-1}$) | $\lambda_{max}$ (nm) |
|---|---|---|---|---|
| MnRe/BPYM | THF | 298 | 2056 m, 2001 s, 1949 vs, 1901 m | 523 |
| | 2-MeTHF | 133 | 2055 m, 1999 s, 1950 sh, 1947 s, 1902 sh, 1896 m | 476 |
| Re(Br)(CO)$_3$(BPYM) | THF | 298 | 2025 s, 1926 m, 1903 m | 384[a] |
| [Re(S)(CO)$_3$(BPYM)]$^\bullet$ | THF | 298 | 2014 s, 1916 s, 1896 s | 474 |
| [Re(S)(CO)$_3$(BPYM)]$^+$ | 2-MeTHF | 133 | 2037 s, 1931 s, 1924 s | 464, 510 |
| | | 173 | 2039 s, 1934 s, 1926 s | |
| [Mn(CO)$_5$]$^-$ | 2-MeTHF | 133 | 1897 s, 1888 sh, 1861 s, 1857 sh | |
| | THF | 298 | 1902 s, 1862 s | |
| Mn(Br)(CO)$_5$ | THF | 298 | 2135 w, 2047 s, 2004 w | |
| Mn$_2$(CO)$_{10}$ | THF | 298 | 2045 m, 2010 s, 1981 w | |
| MnRe/DPP | THF | 298 | 2055 m, 2000 s, 1952 vs, 1901 m | 557 |
| | 2-MeTHF | 133 | 2055, m, 1997 s, 1955 vs, 1895 m | 530 |
| Re(Br)(CO)$_3$(DPP) | THF | 298 | 2023 s, 1925 m, 1902 m | 415 |
| [Re(S)(CO)$_3$(DPP)]$^+$ | 2-MeTHF | 133 | 2035 s, 1932 s, 1923 s | 402, 549 |
| photoproducts MnRe/DPP | | | | |
| **I** | THF | 298 | 2026 m, 2003 s, 1914 s, br, 1891 s, br | |
| **II** | THF | 298 | 2022 s, 1927 m, 1902 m | 510, 650 |
| MnRe/BPYM/Re | THF | 298 | 2060 m, 2030 s, 2007 s, 1958 m, 1936 m, 1917 m | 431, 671 |
| Re(Cl)(CO)$_3$(BPYM)Re(Br)(CO)$_3$ | THF | 298 | 2027 s, 1936 m, 1917 m | |
| [Re(Br)(CO)$_3$]$_2$(BPYM)[b] | THF | 298 | 2024 s, 1936 m, 1912 m | 496 |
| [Re(S)(CO)$_3$(BPYM)Re(Br)(CO)$_3$]$^\bullet$ | THF | 298 | 2028 w, 2015 s, 1917 s, br, 1893 m | 433, 462 |
| | 2-MeTHF | 298 | 2030 w, 2018 s, 1920 s, 1896 m | 389, 466 |
| [(Re(Cl)(CO)$_3$)$_2$(BPYM)]$^{\bullet-}$ [58] | DMF | 298 | | 344, 444, 775 |
| MnRe/DPP/Re | THF | 298 | 2057 m, 2024 s, 2001 s, 1957 m, 1933 m, 1909 m | 474, 636 |
| [Re(Br)(CO)$_3$]$_2$(DPP)[b] | THF | 298 | 2021 s, 1930 m, 1911 m | 455 |
| Re(Cl)(CO)$_3$(DPP)Re(Br)(CO)$_3$ | THF | 298 | 2029 sh, 2021 s, 1933 m, 1911 m | 455 |
| [Re(S)(CO)$_3$(DPP)Re(Br)(CO)$_3$]$^\bullet$ | THF | 298 | 2028 sh, 2020 s, 1931 m, 1910 m | 463 |
| MnRe/BPYM/W | THF | 298 | 2058 m, 2013 m, 2004 s, 1956 s, 1912 s, 1855 m | 450, 684 |
| [Re(S)(CO)$_3$(BPYM)W(CO)$_4$]$^\bullet$ | THF | 298 | 2024 m, 1998 s, 1914 s, br, 1883 s, br, 1836 m | |
| Re(Br)(CO)$_3$(BPYM)W(CO)$_4$[b] | THF | 298 | 2031 m, 2012 s, 1935 m, 1913 s, br, 1896 sh, 1857 m | 444, 634 |

[a] Measured in $CH_3CN$. [b] This work.

**Table 2.** ESR Parameters[a] for the Nitroxides ($t$-Bu)N(O$^\bullet$)Re(CO)$_3$(L) (L = BPYM, DPP, $t$-BuDAB, $i$-Pr-PyCa), [Re(S)(CO)$_3$(L)Re(Br)(CO)$_3$]$^\bullet$, and [Re(S)(CO)$_3$(BPYM)W(CO)$_4$]$^\bullet$ (S = THF)

| complex | $A_{Re}$[a] | $A_{N(NO)}$[a] | $\Delta H_{pp}$[b] |
|---|---|---|---|
| ($t$-Bu)N(O$^\bullet$)Re(CO)$_3$(BPYM)[c] | 28.7 | 15.4 | |
| ($t$-Bu)N(O$^\bullet$)Re(CO)$_3$(DPP)[c] | 29.3 | 15.7 | |
| ($t$-Bu)N(O$^\bullet$)Re(CO)$_3$($t$-BuDAB)[c,43] | 34.9 | 14.01 | |
| ($t$-Bu)N(O$^\bullet$)Re(CO)$_3$($i$-Pr-PyCa)[c,43] | 30.46 | 13.60 | |
| [Re(S)(CO)$_3$(BPYM)Re(Br)(CO)$_3$]$^\bullet$ | | | 52 |
| [(Re(Br)(CO)$_3$)$_2$(BPYM)]$^{\bullet-}$ [57] | 12.0 | | 62 |
| [Re(S)(CO)$_3$(DPP)Re(Br)(CO)$_3$]$^\bullet$ | | | 56 |
| [Re(S)(CO)$_3$(BPYM)W(CO)$_4$]$^\bullet$ | | | 24, 73 |

[a] Coupling constants in gauss. [b] Estimated spectral width in gauss measured as a peak-to-peak separation. [c] Determined from a computer simulation.

was followed *in situ* by IR, UV−vis, and ESR spectroscopies. The IR and UV−vis data for the parent compounds and their photoproducts are collected in Table 1. The photoproducts were characterized by comparing their spectra with those of authentic samples prepared independently or published in the literature. Table 2 presents the ESR parameters of the photoproducts and their adducts with the $t$-BuNO spin trap. Some photoreactions were also studied in 2-MeTHF at 133 K and monitored by IR spectroscopy (Table 1).

**Photochemistry of the Dinuclear Complexes MnRe/L (L = BPYM, DPP).** The MnRe/L complexes were found to react thermally with $CBr_4$ and $CCl_4$ in THF solution to produce Mn(X)(CO)$_5$ and Re(X)(CO)$_3$(L) (X = Br, Cl) as was determined by the IR spectra (see Table 1). On the other hand, both complexes are stable in neat $CH_2Cl_2$ and in THF.

Irradiation of the MnRe/L complexes in $CH_2Cl_2$ into their MLCT absorption bands, i.e. with 514.5 nm light, yielded Mn(Cl)(CO)$_5$ and Re(Cl)(CO)$_3$(L) according to reaction 2.

$$(CO)_5MnRe(CO)_3(L) \xrightarrow[CH_2Cl_2,\ RT]{514.5\ nm} Mn(Cl)(CO)_5 + Re(Cl)(CO)_3(L) \quad (2)$$

The products were characterized by their IR spectra, Table 1. UV−vis spectra monitored during the irradiation exhibited well-developed isosbestic points. Quantum yields of reaction 2 were determined by the disappearance of the MnRe/L starting compounds. Values of 0.36 and 0.54 were found for MnRe/BPYM and MnRe/DPP, respectively. Both quantum yields are temperature-independent over the 258−288 K range. The nature of the products and the analogy with the photochemical behavior of various (CO)$_5$MM′(CO)$_3$(α-diimine) complexes (M, M′ = Mn, Re) studied previously[33−39,48] show that the MnRe/L complexes undergo primary photochemical homolysis of the Mn−Re bond to give [Mn(CO)$_5$]$^\bullet$ and [Re(CO)$_3$(L)]$^\bullet$ radicals that abstract Cl atoms from $CH_2Cl_2$. This was proved independently by performing the photoreaction in neat THF. Irradiation of MnRe/BPYM at 514.5 nm afforded Mn$_2$(CO)$_{10}$, characterized by its typical $\nu$(CO) frequencies,[49] and the [Re(THF)(CO)$_3$(BPYM)]$^\bullet$ radical. The latter species was characterized by comparison of the IR spectra measured during the irradiation with the spectrum of the same species generated independently by spectroelectrochemical reduction of [Re(Otf)(CO)$_3$(BPYM)] in THF.[28] Moreover, *in situ* photolysis of a 5 × 10$^{-4}$M MnRe/BPYM solution in THF in the presence of 5 × 10$^{-3}$ M of the spin trap $t$-BuNO affords the radical adduct $t$-BuN(O$^\bullet$)Re(CO)$_3$(BPYM) whose ESR spectrum is very similar

(48) van der Graaf, T.; van Rooy, A.; Stufkens, D. J.; Oskam, A. *Inorg. Chim. Acta* **1991**, *187*, 133.
(49) Flitcroft, N.; Huggins, D. K.; Kaesz, H. D. *Inorg. Chem.* **1964**, *3*, 1123.

to the spectra found by Andrea[36] for the *t*-BuNO adducts of analogous $[Re(CO)_3(\alpha\text{-diimine})]^\bullet$ radicals. Relevant ESR parameters obtained by a computer simulation of the experimental spectra are summarized in Table 2.

Photochemistry of MnRe/DPP in THF is more complicated. Formation of $Mn_2(CO)_{10}$ and $[Re(THF)(CO)_3(DPP)]^\bullet$ radicals characterized by IR spectroscopy and ESR spectroscopy using *t*-BuNO as a spin trap, respectively, was again found to be the primary photoprocess. However, the IR spectra also revealed the formation of $[Mn(CO)_5]^-$ and of two other unidentified photoproducts **I** and **II** that have $\nu$(CO) frequencies at 2026 m, 2003 s, 1914 s, br, and 1891 s, br $cm^{-1}$ for **I** and at 2022 s, 1927 m and 1902 m $cm^{-1}$ for **II**. Neither of these IR data correspond to the $[Re(THF)(CO)_3(DPP)]^\bullet$ radical, whose $\nu$(CO) frequencies are known from a spectroelectrochemical study.[50] Prolonged irradiation leads to the disappearance of $Mn_2(CO)_{10}$ and of photoproduct **I** with a concomitant increase in the concentration of $[Mn(CO)_5]^-$ and of photoproduct **II**. Apparently, secondary photochemical disproportionation, known[51−54] for many dinuclear carbonyls in coordinating solvents and/or in the presence of Lewis bases, takes place for MnRe/DPP in THF. This secondary photochemistry was not studied further.

Irradiation of MnRe/L complexes at 133 K in 2-MeTHF solutions gave rise to solvent-separated ionic species $[Mn(CO)_5]^-$ and $[Re(2\text{-MeTHF})(CO)_3(L)]^+$, characterized by comparing their IR CO stretching frequencies (Table 1), with those of analogous species.[37,38,55] No evidence for the formation of free CO was found. The starting MnRe/L complexes were fully regenerated upon raising the temperature to 293 K. This photoreactivity strongly resembles that of $[(CO)_4CoMn(CO)_3(BPY)]$[31,56] and of some other $(CO)_5MM'(CO)_3(\alpha\text{-diimine})$ complexes.[31,37,38,55] It undoubtedly involves the formation of strongly reducing photogenerated radicals[36,48] $[Re(2\text{-MeTHF})(CO)_3(L)]^\bullet$, stabilized at low temperature.

**Photochemistry of the Trinuclear Complexes MnRe/L/Re (L = BPYM, DPP) and MnRe/BPYM/W.** The MnRe/BPYM/W and MnRe/DPP/Re complexes were found to react thermally with $CBr_4$ and $CCl_4$ in THF solution. These reactions produced $Mn(X)(CO)_5$ (X = Br, Cl) for both complexes. The other reaction products were identified as $Re(X)(CO)_3(DPP)$-$Re(Br)(CO)_3$ and $Re(X)(CO)_3(BPYM)W(CO)_4$ for the reactions of MnRe/DPP/Re and MnRe/BPYM/W, respectively. The former product was characterized by comparison of its IR spectra with those of $[Re(Br)(CO)_3]_2(DPP)$, which was independently prepared according to literature procedures.[23] To characterize unequivocally the latter product, an authentic sample of $Re(Br)(CO)_3(BPYM)W(CO)_4$ was synthesized independently by stirring equimolar amounts of $Re(Br)(CO)_3$-(BPYM) and $W(CO)_4(Me_3NO)_2$ in THF for one night under a nitrogen atmosphere. Both MnRe/BPYM/W and MnRe/DPP/Re were thermally stable in neat $CH_2Cl_2$ and THF. The MnRe/BPYM/Re complex reacted with $CBr_4$ in THF to produce $Mn(Br)(CO)_5$ and $[Re(Br)(CO)_3]_2(BPYM)$ as was again confirmed by IR spectroscopy. Importantly, MnRe/BPYM/Re does not react thermally with $CCl_4$ in THF solution. To avoid any complications from parallel thermal reactions, the photochemistry of MnRe/DPP/Re and of MnRe/BPYM/W was studied in neat $CH_2Cl_2$. Because of the insolubility of MnRe/BPYM/Re in $CH_2Cl_2$, the photoreactivity of this complex was investigated in THF containing 10% (v:v) $CCl_4$.

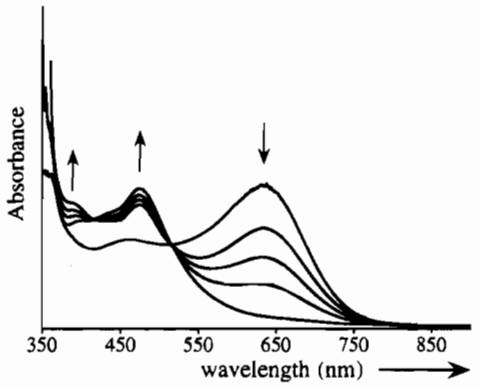


**Figure 2.** UV−vis spectral changes upon photolysis of MnRe/DPP/Re in $CH_2Cl_2$ (room temperature); $\lambda_{exc}$ = 514.5 nm.

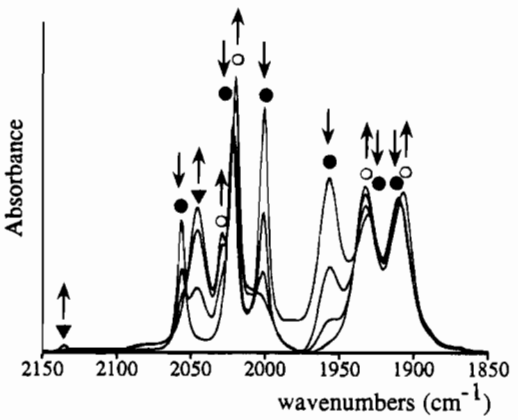


**Figure 3.** IR spectral changes upon photolysis of MnRe/DPP/Re (●) in $CH_2Cl_2$ (room temperature); $\lambda_{exc}$ = 514.5 nm (▼ = $Mn(Cl)(CO)_5$, ○ = $Re(Cl)(CO)_3(DPP)Re(Br)(CO)_3$).

Both MnRe/L/Re (L = BPYM, DPP) and MnRe/BPYM/W were found to be photoreactive in chlorinated solvents. Thus, irradiation of MnRe/DPP/Re with 514.5 nm in $CH_2Cl_2$ yielded $Mn(Cl)(CO)_5$ and $Re(Cl)(CO)_3(DPP)Re(Br)(CO)_3$ according to eq 3. The UV−vis and IR spectral changes accompanying this

$$(CO)_5MnRe(CO)_3(DPP)Re(Br)(CO)_3 \xrightarrow[CH_2Cl_2,\ RT]{h\nu} Mn(Cl)(CO)_5 + Re(Cl)(CO)_3(DPP)Re(Br)(CO)_3 \quad (3)$$

reaction are shown in Figures 2 and 3, respectively. A very similar reaction was observed when MnRe/BPYM/Re was irradiated at 514.5 nm in a $CCl_4$/THF mixture. $Mn(Cl)(CO)_5$ and $Re(Cl)(CO)_3(BPYM)Re(Br)(CO)_3$ were formed:

$$(CO)_5MnRe(CO)_3(BPYM)Re(Br)(CO)_3 \xrightarrow[CCl_4/THF,\ RT]{h\nu} Mn(Cl)(CO)_5 + Re(Cl)(CO)_3(BPYM)Re(Br)(CO)_3 \quad (4)$$

Photolysis of MnRe/BPYM/W at 514.5 nm in $CH_2Cl_2$ produced $Mn_2(CO)_{10}$, together with a product which was not further identified. Products of all these photoreactions were characterized by their IR spectra as was described above. Their character indicates that the trinuclear complexes undergo a photochemical homolysis of the Mn−Re bond, leaving the Re/L/Re or Re/BPYM/W bridged part intact. IR and UV−vis spectra also show that the same products are formed regardless

(50) Stor, G. J.; Hartl, F.; van Outersterp, J. W. M.; Stufkens, D. J. *Organometallics* **1995**, *14*, 1115.
(51) Stufkens, D. J. In *Stereochemistry of Organometallic and Inorganic Compounds*; Bernal, I., Ed.; Elsevier: Amsterdam, 1989; Vol. 3; p 226.
(52) Meyer, T. J.; Caspar, J. V. *Chem. Rev.* **1985**, *85*, 187.
(53) Tyler, D. R. *Prog. Inorg. Chem.* **1988**, *36*, 125.
(54) Tyler, D. R. *Acc. Chem. Res.* **1991**, *24*, 325.
(55) Kokkes, M. W.; Brouwers, A. M. F.; Stufkens, D. J.; Oskam, A. *J. Mol. Struct.* **1984**, *115*, 19.
(56) van Dijk, H. K.; Stufkens, D. J.; Oskam, A. *Inorg. Chem.* **1989**, *28*, 75.

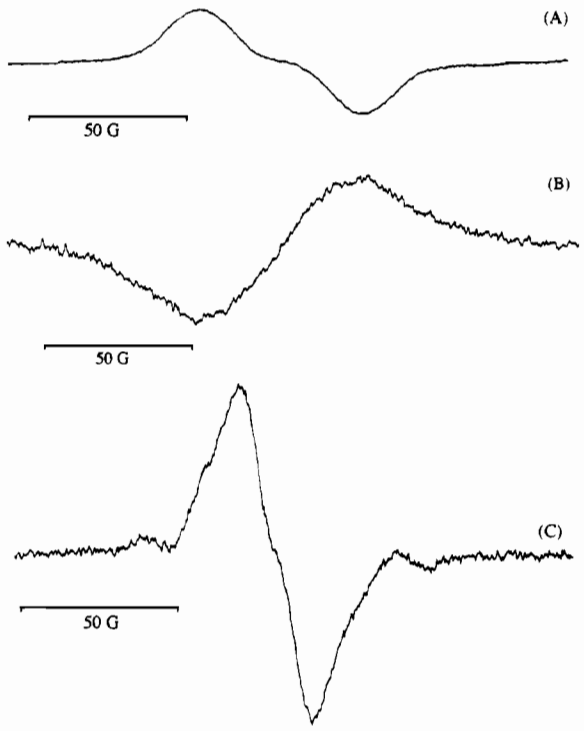


**Figure 4.** ESR spectra in THF at RT after photolysis of (A) MnRe/BPYM/Re, (B) MnRe/DPP/Re, (C) MnRe/BPYM/W; $\lambda_{exc}$ = 514.5 nm.

of the excitation wavelengths varied over the visible spectral region and regardless of the temperature varied over the 288–258 K range.

To further investigate the photoproducts, the photochemistry of the trinuclear complexes was studied also in neat THF. Photolysis of MnRe/L/Re and MnRe/BPYM/W in THF yielded $Mn_2(CO)_{10}$, obviously a product of dimerization of primarily formed $[Mn(CO)_5]^•$ radicals. ESR spectra measured during and after the photolyses proved the radical nature of the other reaction product. The radicals were detectable without using any spin traps. They were found to be stable over 30 min. Their ESR spectra are shown in Figure 4, and corresponding ESR parameters are collected in Table 2. The shape of the ESR spectrum of the MnRe/BPYM/Re photoproduct is similar to that of $[Re(Br)(CO)_3(BPYM)Re(Br)(CO)_3]^{•-}$ reported earlier by Kaim.[57] The width of the photoproduct spectrum ($\Delta H_{pp} \sim 52$ G) is slightly smaller than found for the dimeric radical anion ($\Delta H_{pp} \sim 62$ G).[57] This comparison indicates that the photoproduct has the composition $[Re(THF)(CO)_3(BPYM)Re(Br)(CO)_3]^•$, expected for the product of the homolysis of the Mn–Re bond in MnRe/BPYM/Re. The absence of one $Br^-$ ligand in the photoproduct accounts for the narrower spectral width, as compared with that of the radical anion. The ESR spectrum of the photoproduct obtained from MnRe/DPP/Re has a similar shape and width ($\Delta H_{pp} \sim 56$ G) and was thus assigned to $[Re(THF)(CO)_3(DPP)Re(Br)(CO)_3]^•$. The spectrum of the MnRe/BPYM/W photoproduct (Figure 4) is slightly different, composed of an unresolved line ($\Delta H_{pp}$ = 24 G) with two weak satellites. It could again be assigned to $[Re(THF)(CO)_3(BPYM)W(CO)_4]^•$. The central line corresponds to a molecule containing the ESR-inactive $^{184}W$ (30.7%) and $^{186}W$ (28.6%) isotopes. Since it encompasses the unresolved splitting from only one Re atom, it is much narrower than the signals from the two other photoproducts that contain two Re atoms; vide supra. The satellites correspond to the ESR spectrum of the molecules containing the $^{183}W$ ($I = {}^1/_2$, 14.3%) isotope. The broadness of the signal prevents determination of any splitting constant.

**Table 3.** Quantum Yields[a] (Estimated Error <5%) for the Disappearance of MnRe/DPP/Re in Relation to Temperature and Wavelength of Irradiation[b]

| | $\lambda_{exc}$ (nm) | | | | | | | |
|---|---|---|---|---|---|---|---|---|
| $T$ (K) | 645.0 | 619.7 | 585.0 | 514.5 | 501.7 | 488.0 | 476.5 | 457.9 |
| 288 | 0.24 | 0.25 | 0.32 | 0.37 | 0.38 | 0.38 | 0.41 | 0.45 |
| 278 | 0.22 | | | 0.34 | | | | 0.38 |
| 268 | 0.20 | | | 0.29 | | | | 0.33 |
| 258 | 0.18 | | | 0.25 | | | | 0.30 |
| $E_a$ ($cm^{-1}$) | 494 | | | 695 | | | | 695 |
| $\Phi_0$ | 2.85 | | | 11.89 | | | | 14.35 |

[a] Average values of three measurements. [b] Measured in neat $CH_2Cl_2$.

The remarkable stability of the radical photoproducts in THF solutions allowed the measurement of their UV–vis and IR spectra. The visible absorption spectrum of the MnRe/BPYM/Re photoproduct and that of $[Re(Cl)(CO)_3(BPYM)Re(Cl)(CO)_3]^{•-}$ [58] exhibit bands at 466 and 444 nm, respectively, which have very similar shapes. This type of band is characteristic of a $[BPYM]^{•-}$ ligand-localized radical.[58] The IR spectrum of the photoproduct in the $\nu$(CO) region was measured immediately after the photolysis. The spectral pattern of the frequencies, summarized in Table 1, is similar to that of $Re(Cl)(CO)_3(BPYM)Re(Cl)(CO)_3$. Thus, on the basis of the evidence from ESR, visible, and IR spectra, the photoproduct of MnRe/BPYM/Re in THF is assigned as a dinuclear radical $[Re(THF)(CO)_3(BPYM)Re(Br)(CO)_3]^•$, the unpaired electron being localized mainly on the bridging BPYM ligand. The IR spectrum of this species is very similar to that of the MnRe/DPP/Re photoproduct (Table 1) that was thus assigned as $[Re(THF)(CO)_3(DPP)Re(Br)(CO)_3]^•$. Its IR spectral pattern is, in turn, similar to that exhibited by $[Re(Br)(CO)_3]_2(DPP)$, confirming its assignment. The ESR spectrum of the photoproduct of MnRe/BPYM/W and the similarity between its IR spectrum and that of $Re(Br)(CO)_3(BPYM)W(CO)_4$ (Table 1) are in line with its formulation as $[Re(THF)(CO)_3(BPYM)W(CO)_4]^•$. As expected, the $\nu$(CO) frequencies of the reference nonradical complexes are always somewhat higher than those of the photoproducts which contain the more electron-donating $[BPYM]^{•-}$ or $[DPP]^{•-}$ ligands.

Finally, it should be noted that, at longer irradiation times, the photolyses of the trinuclear species in THF did not proceed isosbestically, probably due to secondary photoreactions of the radical products. All photoreactions studied showed a remarkable temperature effect. At 273 K, the photolyses proceeded significantly more slowly than at 288 K, and no photoreaction was observed in 2-MeTHF at 143 K.

**Quantum Yields for the Photochemical Reaction of the Trinuclear Complexes.** The quantum yields, $\Phi$, of the photoreactions (3) and (4) of MnRe/DPP/Re and MnRe/BPYM/Re were determined in neat $CH_2Cl_2$ and in a 1:10 (v:v%) $CCl_4$/THF mixture, respectively. Quantum yields were studied as a function of the excitation wavelength, $\lambda_{exc}$, and, at several selected $\lambda_{exc}$, also as a function of the temperature. The values measured for MnRe/DPP/Re and MnRe/BPYM/Re are summarized in Tables 3 and 4, respectively. Excitation wavelength dependences are shown in Figure 5. Comparison of the quantum yield data shows that the MnRe/DPP/Re complex is much more reactive than MnRe/BPYM/Re as the $\Phi$ values of the former

(57) Kaim, W.; Kohlmann, S. *Inorg. Chem.* **1990**, *29*, 2909.

(58) Braterman, P. S.; Song, S.-I.; Kohlmann, S.; Vogler, C.; Kaim, W. *J. Organomet. Chem.* **1991**, *411*, 207.

**Table 4.** Quantum Yields[a] (Estimated Error <5%) for the Disappearance of MnRe/BPYM/Re in Relation to Temperature and Wavelength of Irradiation[b]

| | $\lambda_{exc}$ (nm) | | | | | |
|---|---|---|---|---|---|---|
| $T$ (K) | 645.0 | 585.5 | 545.7 | 488.0 | 476.5 | 457.9 |
| 288 | 0.043 | | | 0.053 | | 0.074 |
| 283 | 0.043 | 0.078 | 0.062 | 0.038 | 0.041 | 0.062 |
| 278 | 0.026 | | | 0.025 | | 0.042 |
| 268 | 0.016 | | | 0.014 | | 0.020 |
| 258 | 0.011 | | | 0.006 | | 0.010 |
| $E_a$ (cm$^{-1}$) | 2547 | | | 3695 | | 3578 |
| $\Phi_0$ | $1.45 \times 10^4$ | | | $5.19 \times 10^6$ | | $4.30 \times 10^6$ |

[a] Average values of three measurements. [b] Measured in 1:10 $CCl_4$/THF (v:v, %).

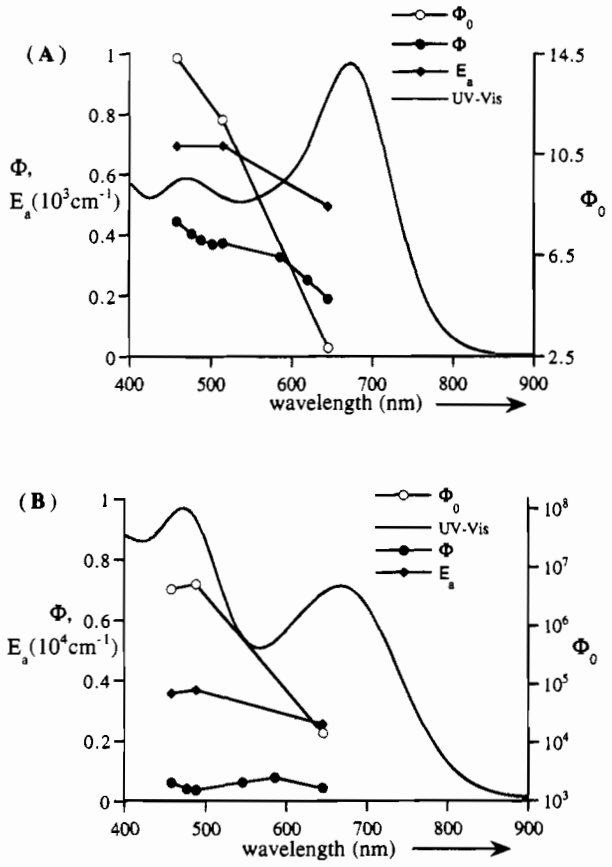


**Figure 5.** Dependence of the quantum yield $\Phi$, the preexponential factor $\Phi_0$, and the activation energy $E_a$ on the excitation wavelength for the homolysis reaction of (A) MnRe/DPP/Re in $CH_2Cl_2$ and (B) MnRe/BPYM/Re in 1:10 (v:v, %) $CCl_4$/THF.

species are about 6 times higher at room temperature. Notably, the room temperature $\Phi$ values of MnRe/DPP/Re dropped by almost 50% when the excitation was tuned from the high-energy into the low-energy absorption band; see Figure 5. The excitation wavelength dependence becomes less pronounced with decreasing temperatures. For the BPYM complex, the $\Phi-\lambda_{exc}$ dependence is less obvious, being almost leveled off at low temperatures.

Within the 258−288 K range studied, the temperature dependence of the quantum yields was always found to follow simple Arrhenius-type behavior described by eq 5. The

$$\Phi = \Phi_0 \exp\left(\frac{-E_a}{RT}\right) \quad (5)$$

experimental data were fitted to this equation with correlation coefficients higher than 0.99. (The only two exceptions were

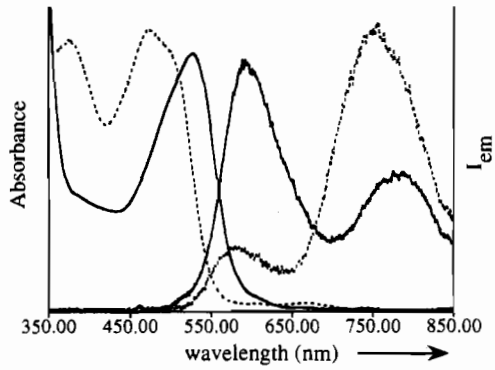


**Figure 6.** Absorption and emission spectra ($\lambda_{exc}$ = 460 nm) of MnRe/BPYM (dashed line) and MnRe/DPP (solid line) in 2-MeTHF at 80 K.

**Table 5.** Emission Properties of MnRe/L (L = BPY, BPYM, DPP), MnRe/DPP/Re, and MnRe/BPYM/W in 2-MeTHF at 80 K

| compound | $\lambda_{exc}$[a] | $\lambda_{max}$ UV−vis[a] | $\lambda_{max,em}$[a] | $\tau$[b] | $10^5\Phi_{em}$[c] |
|---|---|---|---|---|---|
| MnRe/BPY | 460 | 466 | 539 | 2.1 | 0.01 |
| | | | 739 | 6.6 | 0.34 |
| MnRe/BPYM | 460 | 473 | 579 | 0.3 | 3.13 |
| | | | | 1.6 | |
| | | | 739 | 3.7 | 1.61 |
| | 532 | | 739 | 3.1 | |
| MnRe/DPP | 460 | 526 | 589 | 0.6 | 4.27 |
| | | | | 1.6 | |
| | | | 774 | 6.1 | 9.63 |
| | 532 | | 774 | 7.2 | |
| MnRe/DPP/Re | 460 | 588 | 675 | 0.3 | 0.063 |
| | 532 | | 675 | 0.1 | |
| | | | >830 | 0.2 | |
| MnRe/BPYM/W | 460 | 635, 581, 427, 390 | 694, 784 sh | | |

[a] In nm. [b] In $\mu$s (estimated error 10%). [c] Estimated error 25%.

the measurements for MnRe/BPYM/Re at $\lambda_{exc}$ = 645.0 nm and for MnRe/DPP/Re at 457.9 nm, for which the correlation coefficients were 0.981 and 0.988, respectively. However, no systematic deviation from the calculated linear dependences was observed.) The preexponential factors $\Phi_0$ and activation energies $E_a$ are also summarized in Tables 3 and 4, and their excitation wavelength dependences are presented in Figure 5. These data immediately show that the low photoreactivity of MnRe/BPYM/Re relative to MnRe/DPP/Re is caused by a much higher activation energy of the photoreaction of the former complex. Moreover, the decrease of $\Phi$ observed for MnRe/DPP/Re when excited into its low-energy band is a result of a 4−5-fold drop in the preexponential factor $\Phi_0$ that is only partly compensated for by a small decrease in $E_a$; see Figure 5A. Although not evident from the simple $\Phi-\lambda_{exc}$ dependence, MnRe/BPYM/Re exhibits exactly the same behavior (see Figure 5B) with even more pronounced changes in $\Phi_0$ and $E_a$ when excited into the low-energy absorption band.

**Emission Measurements.** Emission spectra of the trinuclear complexes MnRe/L/Re and MnRe/BPYM/W as well as of their dinuclear analogues MnRe/L′ (L′ = BPY, BPYM, DPP) were obtained in a 2-MeTHF glass at 80 K; see Figure 6. Measurements in fluid solutions at higher temperatures were impossible because of efficient photochemical decomposition and decreasing emission intensity. Because of generally low intensities seen at 80 K, no excitation spectra were obtained. Emission data are summarized in Table 5. The emission quantum yields could not be used to calculate $k_r$ and $k_{nr}$ since the efficiency of the population of the non-equilibrated emitting states depended on the wavelength of excitation.

All three dinuclear complexes studied show two emission bands that will hereafter be referred to as the low-energy (LE)

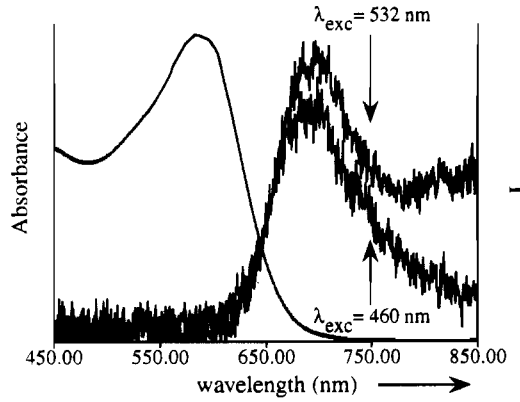


**Figure 7.** Absorption and emission spectra of MnRe/DPP/Re in 2-MeTHF at 80 K. The emission spectra were obtained upon excitation with either 460 nm or 532 nm light.

and high-energy (HE) emissions. The intensity ratio of these two bands is excitation wavelength dependent. For MnRe/BPY and MnRe/BPYM, the LE band in the spectra measured with 460 nm excitation is more intense than the HE band. At 532 nm excitation, the intensity of the HE band diminishes (MnRe/DPP) or the HE band disappears completely (MnRe/BPYM). The HE band is stronger than the LE band in the emission spectrum of MnRe/DPP excited at 460 nm. However, even in this case, the intensity of the HE band decreases strongly when excited at 532 nm. The LE emission always decays monoexponentially with a lifetime of several microseconds, that is, within the experimental error, independent of the excitation wavelength; see Table 5. On the other hand, the decay of the HE emission was found to follow a biexponential kinetics for both MnRe/BPYM and MnRe/DPP; see Table 5. Notably, both the short-lived (hundreds of nanosecond) and the long-lived (about 1.6 $\mu$s) components of the HE emission of both complexes decay considerably faster than the LE emission.

The trinuclear complex MnRe/BPYM/Re is not emissive, even at 80 K. On the other hand, MnRe/DPP/Re showed again a dual luminescence, both emission bands being shifted to lower energies compared with those of its dinuclear MnRe/DPP analogue. The HE band now occurs at 675 nm, whereas the low-energy band extends into the near-IR spectral region, beyond 830 nm, as shown in Figure 7. The emission lifetime found for the HE emission of the trinuclear MnRe/DPP/Re species is smaller by 1 order of magnitude compared with that of MnRe/DPP. Importantly, the LE emission shows up, together with the HE band, only in the spectrum measured after 532 nm excitation. Upon 460 nm excitation, the spectrum is dominated by the HE band, whereas the LE emission occurs, if at all, only as a very weak tail of the HE band. This behavior is opposite to that found for the dinuclear MnRe/DPP species; vide supra.

For MnRe/BPYM/W, only a very weak emission was found at 694 nm. The emission band is asymmetric, with emission intensity slowly decreasing on its high-energy side. No lifetime data have been obtained.

The unstructured band shapes, relatively low energy, and short lifetimes of all the emissions observed suggest that the emissive states are of CT and not intraligand $\pi\pi^*$ character.

## Discussion

The photochemical formation of $Mn_2(CO)_{10}$, the photoreaction with radical scavengers ($CCl_4$, $CH_2Cl_2$), and the detection of the $[Re(CO)_3(L)]^\bullet$ and $[Re(THF)(CO)_3(L)Re(Br)(CO)_3]^\bullet$ radicals clearly show that the homolysis of the Mn−Re bond is the primary photoprocess of both the dinuclear, MnRe/L, and trinuclear, MnRe/L/Re, complexes:

$$(CO)_5MnRe(CO)_3(L) \xrightarrow{h\nu} Mn(CO)_5^\bullet + Re(CO)_3(L)^\bullet \quad (6)$$

$$(CO)_5MnRe(CO)_3(L)Re(Br)(CO)_3 \xrightarrow{h\nu} Mn(CO)_5^\bullet + Re(CO)_3(L)Re(Br)(CO)_3^\bullet \quad (7)$$

Quantum yields of the photoreactions of MnRe/L and MnRe/L/Re were measured in the presence of an excess of the $CH_2Cl_2$ or $CCl_4$ radical scavengers that was large enough to ensure that all the radicals formed were converted into stable products. The quantum yields of the disappearance of the starting complexes may thus be regarded as the quantum yields of the primary photoreactions (6) and (7). Comparison of the excitation wavelength- and temperature-independent quantum yields observed for MnRe/BPYM (0.36) and MnRe/DPP (0.54) with the data for the trinuclear species, presented in Tables 3 and 4, and in Figure 5, shows immediately that the resemblance between the photobehavior of di- and trinuclear complexes is indeed limited to the qualitative nature of their primary photoprocessess (6) and (7) only. Obviously, the attachment of the second metal fragment affects strongly the excited state dynamics that ultimately leads to the photoreaction.

The photoreactivity of the dinuclear complexes MnRe/L parallels that of other $L_nM'M(CO)_3$(α-diimine) complexes (M = Mn, Re; $L_nM'$ = $(CO)_5Mn$, $(CO)_5Re$, $(CO)_4Co$, $Cp(CO)_2Fe$, $Ph_3Sn$).[30-32,36-39,48,56,59] All these species, including the MnRe/L ones described in this paper, undergo efficient M′-M bond homolysis upon irradiation into their low-lying MLCT band. The high quantum yields and their independence of the temperature and excitation wavelength indicate a facile and efficient nonradiative transition from the optically populated MLCT state(s) to the reactive state, that is, most probably, the $^3\sigma\pi^*$ state. This state corresponds to excitation from the orbital that is $\sigma$-bonding with respect to the M′−M (i.e. in the case studied, Mn−Re) bond to the $\pi^*$ orbital of the α-diimine ligand L. Such $^3\sigma\pi^*$ states were originally proposed by Wrighton[30] to be the reactive states of the $(CO)_5M'M(CO)_3$(α-diimine) species. However, the original assignment[30] of the $\sigma \rightarrow \pi^*$ transition as being responsible for the strong absorption in the visible spectral region was later questioned[31,32,60] on the basis of the resonance Raman spectra. Instead, the intense absorption band has been assigned[31,32,38,60] to the excitations into the MLCT states, from which the $^3\sigma\pi^*$ state is populated nonradiatively.[31,32,38] The $^3\sigma\pi^*$ excited states were recently implicated also in the emission and photochemistry of other related complexes $[(CO)_5MnRu(Me)(CO)_2$(α-diimine)$]$,[61,62] $[Re(R)(CO)_3$(α-diimine)$]$,[63] $[Ir(N,Si)_3]$, (N,Si = (6-isopropyl-8-quinolyl)diorganosilyl),[64-66] and $[Ir(R)(CO)(PAr_3)_2(mnt)]$.[67]

Thus, the photochemical and photophysical behaviors of the MnRe/L complexes may readily be explained (see Scheme 1)

(59) Servaas, P. C.; Stor, G. J.; Stufkens, D. J.; Oskam, A. *Inorg. Chim. Acta* **1990**, *178*, 185.
(60) Kokkes, M. W.; Snoeck, T. L.; Stufkens, D. J.; Oskam, A.; Cristophersen, M.; Stam, C. H. *J. Mol. Struct.* **1985**, *131*, 11.
(61) Nieuwenhuis, H. A.; Stufkens, D. J.; Oskam, A. *Inorg. Chem.* **1994**, *33*, 3212.
(62) Nieuwenhuis, H. A.; Stufkens, D. J.; Vlček,, A., Jr. *Inorg. Chem.* **1995**, *34*, 3879.
(63) Rossenaar, B. D.; Kleverlaan, C. J.; Stufkens, D. J.; Oskam, A. *J. Chem. Soc., Chem. Commun.* **1994**, 63.
(64) Djurovich, P. I.; Watts, R. J. *Inorg. Chem.* **1993**, *32*, 4681.
(65) Djurovich, P. I.; Watts, R. J. *J. Phys. Chem.* **1994**, *98*, 396.
(66) Djurovich, P. I.; Cook, W.; Joshi, R.; Watts, R. J. *J. Phys. Chem.* **1994**, *98*, 398.
(67) Bradley, P.; Suardi, G.; Zipp, A. P.; Eisenberg, R. *J. Am. Chem. Soc.* **1994**, *116*, 2859.

**Scheme 1.** Excited State Dynamics Relevant to the Photochemistry and Emission of the Dinuclear MnRe/L Complexes[a]

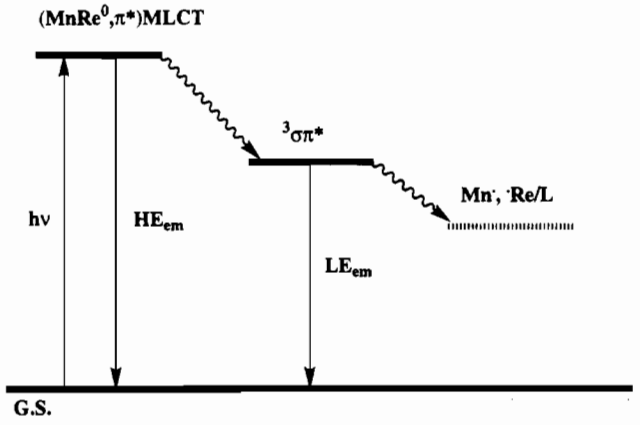


[a] To keep the scheme simple, neither the spin-singlet and -triplet MLCT manifolds nor their individual component states are distinguished. The $^1\sigma\pi^*$ state is also not shown.

as involving a manifold of closely spaced MLCT states, which may be populated optically, and a low-lying $^3\sigma\pi^*$ state, which is reactive with respect to homolysis of the Mn−Re bond. (The MLCT manifold comprises states arising from the excitations from different d($\pi$) orbitals of the $(CO)_5MnRe(CO)_3$ fragment to the $\pi^*$(LUMO). Hereafter, the notation ($MnRe^0$,$\pi^*$)MLCT state and ($MnRe^0 \rightarrow \pi^*$)MLCT transition will be used.) Observation of a multiple emission indicates that, at 80 K, the emitting excited states are not thermally equilibrated. The high-energy (HE) emission is assigned to the ($MnRe^0$,$\pi^*$)MLCT manifold, in accord with previous results obtained on analogous dinuclear complexes.[34,35] The biexponential decay of the HE emission, observed for both MnRe/BPYM and MnRe/DPP, clearly indicates the presence of at least two emitting levels, presumably corresponding to individual members of the spin-triplet MLCT manifold, as suggested by the relatively long lifetimes; see Table 5. The low-energy (LE) emission occurs at energies lower by some 1000 $cm^{-1}$ than the HE emission. Importantly, its lifetime, 3.4 $\mu$s for MnRe/BPYM and 6.7 $\mu$s for MnRe/DPP, is significantly longer even than the longer lifetime of the biexponential decay of the HE, i.e. MLCT, emission of both complexes, 1.6 $\mu$s. It is also larger than the MLCT emission lifetime found for the mononuclear complexes $Re(Cl)(CO)_3(DPP)$[11] and $Re(Cl)(CO)_3(BPYM)$[21] (0.76 and 0.22 $\mu$s, respectively). The increase of the lifetime with a large decrease in emission energy upon going from the HE to the LE emission is opposite to the prediction based on the energy gap law, indicating that the HE and LE emissions originate from excited states of different orbital parentages. Hence, the LE emission may be, for all three MnRe/L′ complexes studied (L′ = BPY, BPYM, DPP), assigned to the emission from the $^3\sigma\pi^*$ state. A similar, relatively long-lived, low-energy $^3\sigma\pi^*$ emission was recently observed for analogous $(CO)_5MnRu(R)(CO)_2$(α-diimine) compounds,[62] and long $^3\sigma\pi^*$ lifetimes have been found for other complexes as well.[63−67] Interestingly, the HE emission strongly diminishes in intensity, or even disappears, when the excitation energy is tuned from 460 to 532 nm. For all three complexes investigated, this means changing the excitation from the high-energy side to the low-energy side of the MLCT absorption band. In fact, the shape of the absorption spectra measured at 80 K clearly reveals that the absorption band consists of at least two components; see Figure 6. The 460 and 532 nm excitations are thus directed into different MLCT transitions. The excitation wavelength dependence of the HE/LE intensity ratio, i.e. the relative decrease of the HE-band intensity with increasing excitation wavelength, then suggests either (i) that the lower-lying member(s) of the MLCT manifold is (are) less emissive and/or converted (at 80 K) to $^3\sigma\pi^*$ faster than the higher MLCT levels or (ii) that the $\sigma \rightarrow \pi^*$ electronic transition contributes to the low-energy side of the MLCT absorption band, into which the 532 nm excitation was directed. In any case, the observation of an emission from the $^3\sigma\pi^*$ state upon ($MnRe^0 \rightarrow \pi^*$)MLCT excitation shows that the ($MnRe^0$,$\pi^*$)MLCT $\rightarrow$ $^3\sigma\pi^*$ nonradiative transition is rather efficient, even at 80 K.

The attachment of the $Re^I(Br)(CO)_3$ group to the free N atoms of the ligand L in MnRe/L complexes stabilizes[26] the $\pi^*$-LUMO of the bridging ligand L by approximately 5000 $cm^{-1}$ for MnRe/BPYM and 3150 $cm^{-1}$ for MnRe/DPP, as was manifested by the positive shifts of the reduction potentials, +0.62 and +0.39 V, respectively, measured in butyronitrile at 213 K.[27,28] This stabilization of the $\pi^*$ orbital results also in a shift of the ($MnRe^0 \rightarrow \pi^*$)MLCT transitions upon formation of the trinuclear bridged species by 4510 $cm^{-1}$ for MnRe/BPYM and by 1990 $cm^{-1}$ for MnRe/DPP, as measured in $CH_3CN$.[68] Smaller spectral than electrochemical shifts indicate that the d($\pi$) orbitals of the $MnRe^0$ fragment are stabilized as well, although to a much smaller extent than the $\pi^*$. Stabilization by 490 $cm^{-1}$ and by 1160 $cm^{-1}$ may be estimated for MnRe/BPYM/Re and MnRe/DPP/Re, respectively. The reactive state $^3\sigma\pi^*$ is not accessible to direct spectroscopic observation. However, it is expected to be also strongly stabilized by the attachment of the $Re^I(Br)(CO)_3$ group due to the stabilization of the $\pi^*$ level. Moreover, the energy of the $\sigma$ orbital (essentially a $d_{z^2}(Mn^0) + d_{z^2}(Re^0)$ combination), which does not interact directly with the orbitals of the bridging ligand L, is not expected to be much affected by the formation of the bridged species. Thus, the $^3\sigma\pi^*$ state of the MnRe/L group in MnRe/L/Re will be stabilized relative to the dinuclear MnRe/L species by the same amount as the $\pi^*$ orbital, i.e. by about 5000 $cm^{-1}$ for BPYM and by about 3150 $cm^{-1}$ for DPP. This comparison also implies that the energy gap between the ($MnRe^0$,$\pi^*$)MLCT and the $\sigma\pi^*$ states will be larger in the trinuclear than in the dinuclear complexes. The energy difference between the ($MnRe^0$,$\pi^*$)MLCT and $^3\sigma\pi^*$ state is expected to be some 600 $cm^{-1}$ larger for the MnRe/DPP/Re than for the MnRe/BPYM/Re complex because of a larger d($\pi$) stabilization in the former species; vide supra.

Besides the $\pi^*$-orbital stabilization, the attachment of the $Re^I(Br)(CO)_3$ group also introduces another manifold of MLCT transitions from the d($\pi$) orbitals of $Re^I(Br)(CO)_3$ to the $\pi^*$-LUMO of the bridging ligand L.[26] Our recent investigations of the electronic absorption and resonance Raman spectra of the MnRe/L/Re complexes[26] have clearly shown that the electronic interaction between the $MnRe^0$ and the $Re^I$ centers is rather small both in the ground state and in the MLCT excited states originating from either the $MnRe^0$ or the $Re^I$ group. Therefore, the low- and high-energy MLCT bands have distinct $MnRe^0 \rightarrow \pi^*$ and $Re^I \rightarrow \pi^*$ localized MLCT characters, respectively.[26]

The above discussion suggests that the photochemistry and emission of the trinuclear MnRe/L/Re complexes may be discussed in terms of three, essentially localized, excited states: ($Re^I$,$\pi^*$)MLCT, ($MnRe^0$,$\pi^*$)MLCT, and $^3\sigma\pi^*$; see Scheme 2. Interestingly, the homolysis of the Mn−Re bond still occurs in the MnRe/L/Re complexes upon ($MnRe^0 \rightarrow \pi^*$)-MLCT excitation, although no longer as a barrierless temper-

(68) The energies of the MLCT maxima are solvent dependent.[26] However, the general trends are the same in all solvents studied. For example, going from MnRe/L to MnRe/L/Re, the ($MnRe \rightarrow \pi^*$)MLCT absorption band measured in the 2-MeTHF glass at 80 K shifts by −4100 $cm^{-1}$ for L = BPYM and by −2000 $cm^{-1}$ for DPP.

**Scheme 2.** Excited State Dynamics Relevant to the Photochemistry of the Trinuclear Complexes[a]

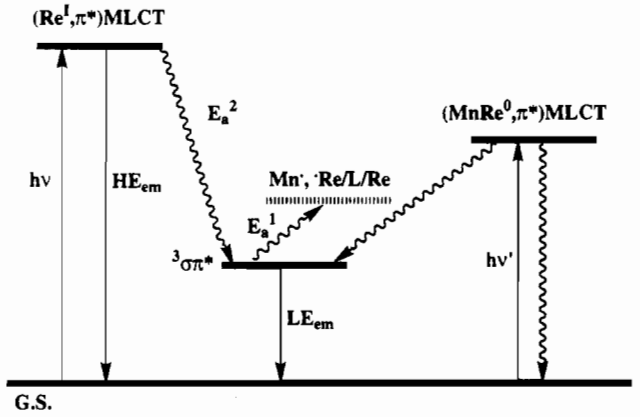


[a] The reactive $^3\sigma\pi^*$ state is shown at lower energy than the dissociated state to stress that the Mn−Re bond homolysis is, because of low $^3\sigma\pi^*$-state energy, an activated process, $E_a^1$. The $^3\sigma\pi^*$ state is populated by two independent pathways either from (Re$^I$,π*)MLCT (activated, $E_a^2$) or from (MnRe$^0$,π*)MLCT states depending on the excitation energy, $h\nu$ or $h\nu'$, respectively. The deactivation of the (MnRe$^0$,π*)MLCT state is relatively fast, competing efficiently with the conversion to the $^3\sigma\pi^*$ state. (Neither spin-singlet and -triplet manifolds nor their individual component states are distinguished. The $^1\sigma\pi^*$ state is not shown.

ature-independent process as was the case for the dinuclear MnRe/L species. The observation that the attachment of the Re$^I$(Br)(CO)$_3$ group to the MnRe/L species introduces an energy barrier into the Mn−Re photodissociation upon (MnRe$^0$ → π*)-MLCT excitation is rather surprising, for the reactive $^3\sigma\pi^*$ state is still the lowest-lying state and neither the nature nor the frequencies of the vibrations that couple the (MnRe$^0$,π*)MLCT and $^3\sigma\pi^*$ excited states are expected to be much different in the di- and trinuclear species. Hence, the activation energy found for the MnRe/L/Re species is not supposed to be related to the (MnRe$^0$,π*)MLCT → $^3\sigma\pi^*$ nonradiative transition. However, the stabilization of the $^3\sigma\pi^*$ state upon formation of the bridged trinuclear complexes may bring it well below the energy needed to form the {[(CO)$_5$Mn]•, [Re(CO)$_3$(L)Re(Br)-(CO)$_3$]•} dissociated state. Hence, an activation energy would be needed to bring about the dissociation of the Mn−Re bond from the low-lying $^3\sigma\pi^*$ state of MnRe/L/Re. In accord with this explanation, the activation energy found for the photoreaction induced by the (MnRe$^0$ → π*)MLCT excitation increases with increasing stabilization of the π* orbital and, hence, of the $^3\sigma\pi^*$ state upon formation of the trinuclear complexes. Thus, the estimated $^3\sigma\pi^*$ stabilization by 5000 cm$^{-1}$ in MnRe/BPYM/Re and by 3150 cm$^{-1}$ in MnRe/DPP/Re may well account for the activation energies of about 2550 and 500 cm$^{-1}$, respectively, that were measured experimentally using the excitation into the lowest (MnRe$^0$,π*)MLCT absorption band of these complexes; see Tables 3 and 4 and Figure 5. Similar effects were observed in the photochemistry[69] of Os$_3$(CO)$_{10}$(L) and Os$_3$(CO)$_{10}$(L)Re-(Br)(CO)$_3$ clusters.

Excitation into the higher (Re$^I$,π*)MLCT state also induces homolysis of the Mn−Re bond that occurs with higher quantum yields than under the (MnRe$^0$ → π*)MLCT excitation; see Tables 3 and 4 and Figure 5. However, for both MnRe/BPYM/Re and MnRe/DPP/Re, the activation energy observed upon the higher (Re$^I$ → π*)MLCT excitation is larger than the activation energy needed for the dissociation of the Mn−Re bond in the $^3\sigma\pi^*$ state, which was measured with the lower (MnRe$^0$ → π*) MLCT excitation; vide supra. This extra activation energy, 200 cm$^{-1}$ for MnRe/DPP/Re and 1100 cm$^{-1}$ for MnRe/BPYM/Re, observed with high-energy excitation, has thus to be associated with the nonradiative population of the reactive $^3\sigma\pi^*$ state from the (Re$^I$,π*)MLCT state. As follows from Scheme 2, the $^3\sigma\pi^*$ state might be populated either by a direct nonradiative transition (Re$^I$,π*)MLCT → $^3\sigma\pi^*$ or by a stepwise process (Re$^I$,π*)MLCT → (MnRe$^0$,π*)MLCT → $^3\sigma\pi^*$. The very fact that the photochemical quantum yields are higher for the higher (Re$^I$ → π*)MLCT excitation than for the reaction starting from the lower (MnRe$^0$,π*)MLCT state alone (see Tables 3 and 4 and Figure 5) clearly favors the former, direct transition.

The photochemical behavior of MnRe/L/Re thus indicates that the rate of the (Re$^I$,π*)MLCT → (MnRe$^0$,π*)MLCT nonradiative transition is lower than the rate of the (Re$^I$,π*) → $^3\sigma\pi^*$ transition. This striking observation may be understood by taking into account that the two MLCT states are confined to separate parts of the molecule, adjacent to the metal centers from which the MLCT transitions originate.[26] Formally, the (Re$^I$,π*)MLCT state may be viewed as MnRe$^0$/L$^-$/Re$^{II}$ and the (MnRe$^0$,π*)MLCT state as MnRe$^I$/L$^-$/Re$^I$. As was indicated by resonance Raman spectroscopy,[26] each of these localized excitations activates mainly the localized vibrations of the bonds within those chelate rings that include the metal atom from which the electron is actually excited. The ν(CO) vibrations of the (CO)$_5$MnRe(CO)$_3$ and Re(Br)(CO)$_3$ fragments are also activated separately by the (MnRe$^0$ → π*)MLCT and (Re$^I$ → π*)MLCT excitations, respectively.[26] For MnRe/BPYM/Re, even the C−N bond vibrations within the BPYM ligand that are adjacent to the (CO)$_5$MnRe(CO)$_3$ and Re(Br)(CO)$_3$ groups are activated separately by the (MnRe$^0$ → π*)MLCT and (Re$^I$ → π*)MLCT excitations, respectively.[26] Hence, the lack of a vibration that would be strongly coupled to both MLCT states might be responsible for the relatively slow rate of the (Re$^I$,π*)-MLCT → (MnRe$^0$,π*)MLCT nonradiative transition. Moreover, the electronic interaction between the two metal centers has been found to be rather weak in the ground state as well as in both MLCT states.[26] This would further diminish the rate of the electron transfer from the d(π) orbital of the MnRe$^0$ unit to the d(π) orbital of the "oxidized" Re$^{II}$(Br)(CO)$_3$ group through the "reduced" bridging ligand L$^{\bullet-}$ that is needed to accomplish the (Re$^I$,π*)MLCT → (MnRe$^0$,π*)MLCT nonradiative transition. On the other hand, the (Re$^I$,π*)MLCT → $^3\sigma\pi^*$ nonradiative transition amounts to an electron transfer from the Mn−Re σ orbital which is oriented perpendicularly to the Re$^0$/L/Re$^I$ plane (Figure 1), to the d(π) orbital of the Re(Br)(CO)$_3$ unit, also located above and below the Re$^0$/L/Re$^I$ plane. Because of the short distance, a through-space electron transfer can easily be envisaged. Alternatively, the hole-transfer superexchange mechanism through the σ bonds might also operate. Electronic coupling through σ bonds is known to be rather efficient both for BPYM[70] and for the pyrazine ring[25,71] present in the DPP ligand. Whatever mechanism is actually dominant, the (Re$^I$,π*)-MLCT → $^3\sigma\pi^*$ transition is expected to be faster in MnRe/DPP/Re than in MnRe/BPYM/Re as the necessarily nonplanar configuration of the DPP bridge[6] breaks down the σ/π orthogonality and also makes the through-space overlap more favorable.

To account for the fact that the estimated "extra" activation energy associated with the population of the $^3\sigma\pi^*$ state from the (Re$^I$,π*)MLCT state is much lower (200 cm$^{-1}$) for MnRe/DPP/Re than for MnRe/BPYM/Re (1100 cm$^{-1}$), let us consider

(69) van Outersterp, J. W. M.; Garriga Oostenbrink, M. T.; Hartl, F.; Nieuwenhuis, H. A.; Stufkens, D. J. *Inorg. Chem.*, in press.

(70) Castro, I.; Sletten, J.; Glaerum, L. K.; Lloret, F.; Faus, J.; Julve, M. *J. Chem. Soc., Dalton Trans.* **1994**, 2777.

(71) Hay, P. J.; Thibeault, J. C.; Hoffmann, R. *J. Am. Chem. Soc.* **1975**, *97*, 4884.

**Scheme 3.** Potential Energy Curves of the ($Re^I,\pi^*$)MLCT, ($MnRe^0,\pi^*$)MLCT, and $^3\sigma\pi^*$ Excited States in MnRe/L/Re[a]

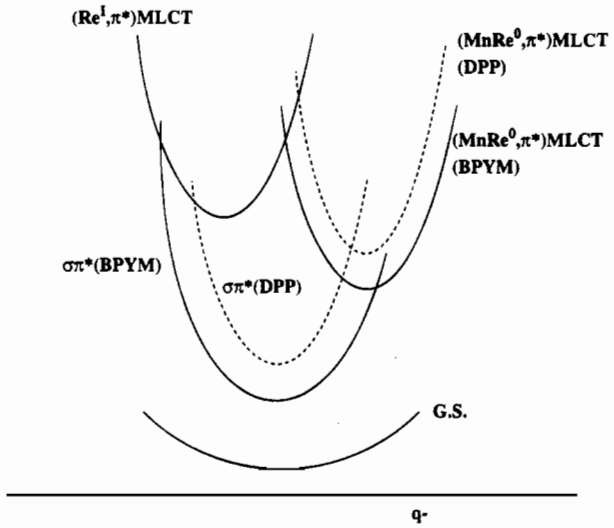


[a] Dashed lines are for L = DPP; solid lines are for L = BPYM. The curves are schematically shown against an asymmetric coordinate,[73] $q$-, that reflects the differences in the coordination environments (mainly the Re−N bond lengths) around the Re atoms in the $(CO)_5MnRe(CO)_3$ and $Re(Br)(CO)_3$ groups. Whereas the MLCT states are significantly displaced with respect to this coordinate, the displacement of the $^3\sigma\pi^*$ state, which occurs in the same direction as for the ($MnRe^0,\pi^*$)MLCT state, is much smaller, as the $\sigma$ orbital is not involved directly in the bonding to the ligand L. The origins of the energy barriers for the ($Re^I,\pi^*$)MLCT → $^3\sigma\pi^*$ and ($Re^I,\pi^*$)MLCT → ($MnRe^0,\pi^*$)MLCT conversions are shown as well. The barrier for the latter process is rather large because of the different localizations and, hence, large relative displacement of the two MLCT states involved. Whereas ($Re^I,\pi^*$)MLCT occurs at comparable energies for both L = BPYM and L = DPP, the energies of the $^3\sigma\pi^*$ and ($MnRe^0,\pi^*$)MLCT states are much lower for BPYM than for DPP; see the text.

that the ($Re^I \rightarrow \pi^*$)MLCT transition occurs at about the same energy for both MnRe/DPP/Re and MnRe/BPYM/Re, regardless the medium in which the absorption spectra were obtained.[26] However, the $^3\sigma\pi^*$ state lies much lower in energy for MnRe/BPYM/Re, as was discussed in the preceding paragraphs. Hence, the energy gap between the ($Re^I,\pi^*$)MLCT and the $\sigma\pi^*$ states should be much higher in MnRe/BPYM/Re than in MnRe/DPP/Re. As follows from the necessarily "inverted" character of the ($Re^I,\pi^*$)MLCT → $^3\sigma\pi^*$ nonradiative transition (see Scheme 3), the higher energy gap translates into higher apparent activation energy expected for MnRe/BPYM/Re. For the latter complex, another contribution to the activation energy might originate from the reorganizational energy needed to adjust the large asymmetric distortion of the BPYM ligand that appears to be different in different excited states.[26]

Despite the higher activation energy, the Mn−Re homolysis occurs, within the temperature range studied, with a higher or comparable overall quantum yield when it originates from the ($Re^I,\pi^*$)MLCT state relative to the reaction from the ($MnRe^0,\pi^*$)-MLCT state. This is possible because of a large decrease of the preexponential factor $\Phi_0$ upon changing the excitation from the ($Re^I \rightarrow \pi^*$)MLCT absorption band to the lower energy ($MnRe^0 \rightarrow \pi^*$)MLCT band; see Figure 5. The much lower preexponential factor observed for the reaction from the low-lying ($MnRe^0,\pi^*$)MLCT state is probably caused[72] by its very rapid competitive nonradiative deactivation to the ground state, whose rate essentially follows the energy gap law. Therefore the unproductive deactivation of the ($MnRe^0,\pi^*$)MLCT state is expected to be much faster than that of the higher ($Re^I,\pi^*$)-MLCT state. For the same reason, the ($MnRe^0,\pi^*$)MLCT deactivation plays a much larger role in MnRe/L/Re than in the MnRe/L complexes.

The above explanation of the photoreactivity also accounts for the unusual observation that the low-energy emission from MnRe/DPP/Re is observable (Figure 7) only upon 532 nm excitation into the lower ($MnRe^0 \rightarrow \pi^*$) absorption band, not when the excitation is directed into the higher ($Re^I \rightarrow \pi^*$)MLCT transition using 460 nm light. On the other hand, the high-energy emission is observed at both 460 and 532 nm excitations. As follows from the low-temperature spectrum shown in Figure 7, the two absorption bands of MnRe/DPP/Re partly overlap. Whereas the 460 nm excitation is mostly directed to the higher ($Re^I \rightarrow \pi^*$)MLCT absorption band, the 532 nm light actually excites both the ($Re^I \rightarrow \pi^*$) and ($MnRe^0 \rightarrow \pi^*$)MLCT transitions simultaneously. Hence, the HE emission, observed at both excitations, is assigned to the ($Re^I,\pi^*$)MLCT excited state, as in the case of the emission observed[11,13] from [Re(Cl)-$(CO)_3]_2$(DPP) that emits[11] at 690 nm, $\tau$ =280 ns (EtOH glass, 77 K). The somewhat shorter lifetime (~100 ns) found for MnRe/DPP/Re is undoubtfully a consequence of an asymmetric, and thus more distorted,[26] coordination of the DPP ligand. Importantly, neither the $^3\sigma\pi^*$ nor the ($MnRe^0,\pi^*$)MLCT excited state may be populated nonradiatively from the ($Re^I,\pi^*$)MLCT state at a temperature as low as 80 K which does not allow us to surmount the associated energy barriers whose presence has been deduced from the photochemical experiments. On the other hand, the excitation at 532 nm partly populates also the lower ($MnRe^0,\pi^*$)MLCT state which undergoes an activationless nonradiative transition to the low-lying $^3\sigma\pi^*$ state even at 80 K, as follows from the emission properties of the dinuclear MnRe/L complexes; vide supra. The LE emission of MnRe/DPP/Re (whose maximum occurs in the near-IR spectral region) was assigned, as for the dinuclear MnRe/L species, to the $^3\sigma\pi^*$ state. This assignment is fully supported by the characteristic[32,33,62−67] long lifetime (200 ns) of the LE emission, which is even longer than the lifetime of the HE, $^3$($Re^I,\pi^*$)MLCT emission (100 ns). This comparison effectively rules out an alternative asignment of the LE emission to the $^3$($MnRe^0,\pi^*$)-MLCT state, for which a lifetime shorter than that of the HE emission is expected on the basis of the energy gap law. The ($MnRe^0,\pi^*$)MLCT state is nonemissive, probably because of its fast nonradiative deactivation both to the $^3\sigma\pi^*$ state and to the ground state.

The lack of any emission from MnRe/BPYM/Re is not unusual. The BPYM-bridged complexes are generally much less emissive or even not emissive at all while their DPP analogues emit.[6,7,11,20,21] In the case of MnRe/BPYM/Re, the lack of emission may be related to even lower energies of the relevant excited states and to their stronger nonradiative coupling to the ground state, presumably as a consequence of a significant BPYM ligand distortion.[26]

## Conclusions

The dinuclear MnRe/L complexes (L = BPYM, DPP) undergo efficient photochemical homolysis of the Mn−Re bond when excited into the ($MnRe^0 \rightarrow \pi^*$)MLCT transition. It is an activationless process that occurs from the $^3\sigma\pi^*$ state, which is

(72) The preexponential factor $\Phi_0$ is a rather complex quantity, dependent on several rate constants involved. However, it is generally expected to decrease with increasing rate of an unproductive competitive deactivation of any of the excited states involved in the photochemical pathway. Otherwise, because of the complexity of this parameter, we refrain from its more detailed discussion, especially from comparisons of its values obtained for different molecules.

(73) Wong, K. Y.; Schatz, P. N. *Prog. Inorg. Chem.* **1981**, *28*, 369.

efficiently nonradiatively populated from the optically excited MLCT state. Both the MLCT and the $^3\sigma\pi^*$ states are emissive at 80 K.

Attachment of the $Re(Br)(CO)_3$ group to the uncoordinated N atoms of the potentially bridging ligand L strongly stabilizes both the ($MnRe^0$,$\pi^*$)MLCT and $^3\sigma\pi^*$ states and introduces a new ($Re^I$,$\pi^*$)MLCT state into the resulting trinuclear MnRe/L/Re molecules. The reactive $^3\sigma\pi^*$ state is shifted in energy below the dissociated state, making the Mn−Re bond homolysis from the $^3\sigma\pi^*$ state an activated process. This effect is larger for the BPYM than for the DPP complex because of a greater stabilization of the $\pi^*$ BPYM orbital. The reactive $^3\sigma\pi^*$ state in MnRe/L/Re is populated by two independent pathways, either from the higher ($Re^I$,$\pi^*$)MLCT state or from the lower ($MnRe^0$,$\pi^*$)MLCT state, depending on the excitation energy. The ($Re^I$,$\pi^*$)MLCT → $^3\sigma\pi^*$ conversion is a relatively efficient process that, however, requires an activation energy, apparently resulting from its "inverted" character. The efficiency of the ($MnRe^0$,$\pi^*$)MLCT → $^3\sigma\pi^*$ transition is diminished in comparison with that of the dinuclear MnRe/L complexes by a faster competitive nonradiative transition of the ($MnRe^0$,$\pi^*$)MLCT state caused by the lowering of its energy. The conversion between the two MLCT excited states is relatively inefficient, not contributing to the photochemistry observed.

This study shows that photochemical bond activation is quite possible even in bridged polynuclear complexes, unless the unproductive deactivation of the optically excited MLCT states becomes too competitive with their conversion into the reactive state and, especially, unless the reactive, usually $^3\sigma\pi^*$, state is not stabilized too much below the energy of the bond to be activated.

**Acknowledgment.** The Netherlands Foundation for Chemical Research (SON), the Netherlands Organisation for Pure Research (NWO), and the European COST Program are thanked for financial support. A.V. acknowledges financial support from the Granting Agency of the Czech Republic (Grant no. 203/93/0250).

IC950158Y